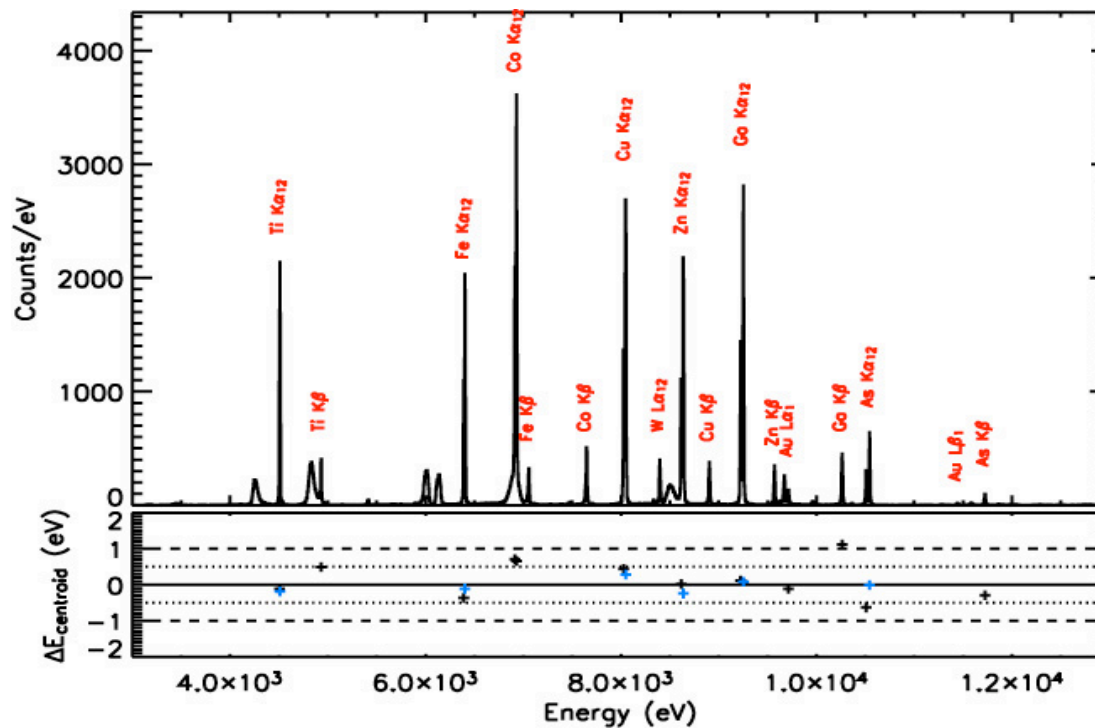

XRS Calibration

Status & In-Flight Plan

- **Energy Scale**
 - **Line Spread Function**
 - **Effective Area**
 - **Background**
-

Energy Scale

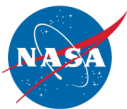
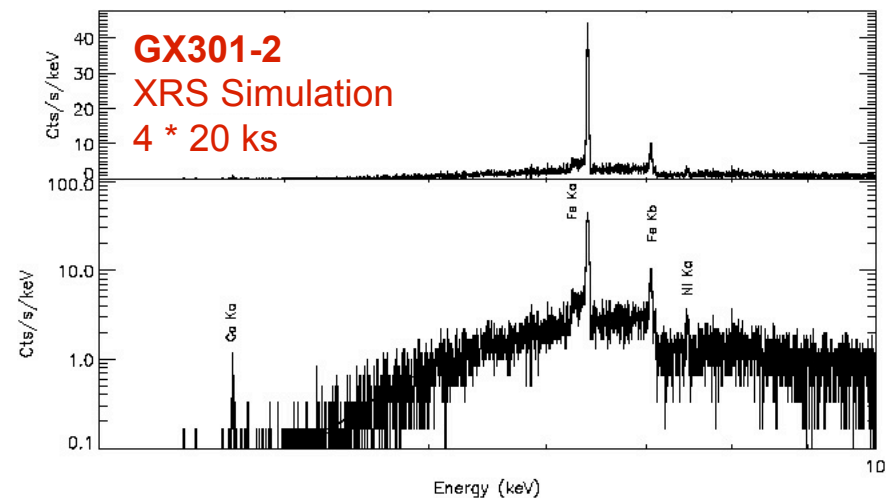
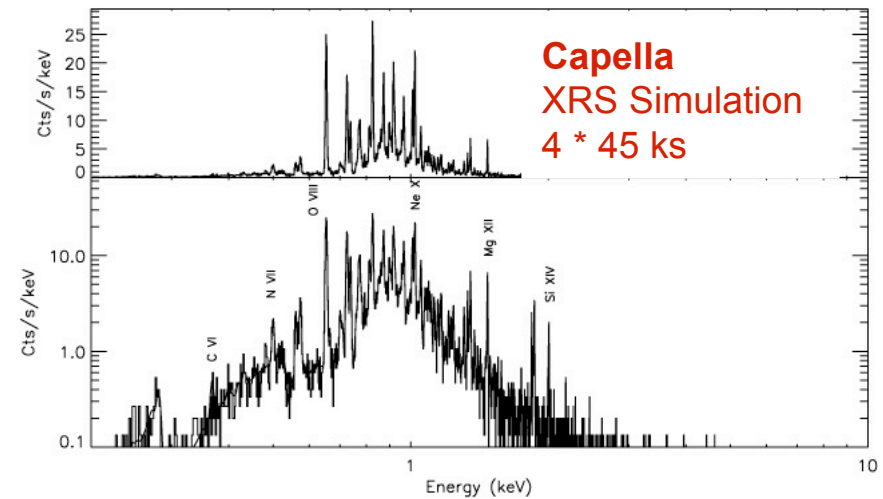
The energy scale is a complicated, non-analytic function. Using a physical model for the pulses, we find that $E(V)$ can be well characterized by a 4th order polynomial. For ground calibration data this gives an energy scale that is accurate to $\Delta E \lesssim 0.5 \text{ eV}$



Energy Scale: In-Flight

The energy scale must be re-established in-flight. We will use offset pointings of **Capella** and **GX301-2** to illuminate all pixels.

Line	Energy (keV)	Inner Pixel	Outer Pixel
N VII Ly α	0.500	105	58
O VIII Ly α	0.654	1045	404
Ne X Ly α	1.022	1051	407
Mg XII Ly α	1.473	279	108
Si XIV Ly α	2.006	70	27
K K α	3.314	186	186
Mn K α	5.894	6200	6200
Fe K α	6.400	3320	1262
Ni K α	7.461	105	40



Energy Scale: Drift Correction

Changes in the energy scale will be tracked using an offset pixel.

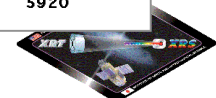
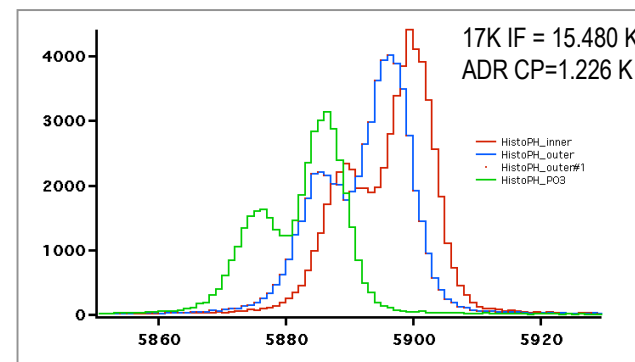
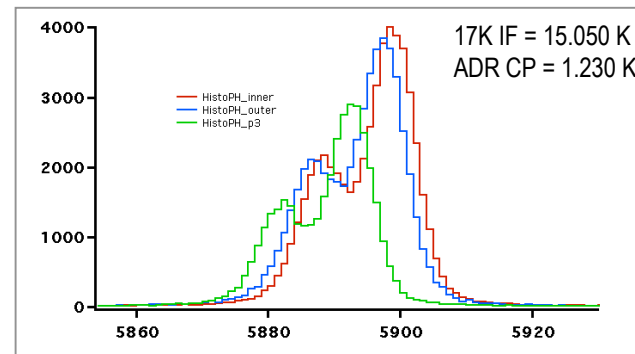
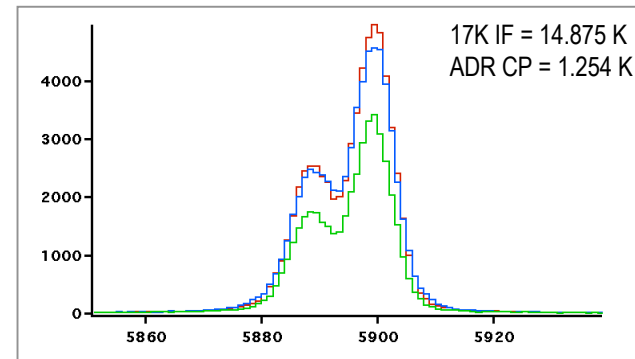
During ground calibration we discovered that the calibration pixel and the array pixels respond differently to changes in the thermal environment.

This is very difficult to characterize. For small changes in temperature, the drift is linear.

Cal Pixel:

$$\Delta T_{\text{Ne}} \sim 40 \text{ eV/K}$$

$$\Delta T_{\text{He}} \sim 130 \text{ eV/K}$$



Line Spread Function

The line spread function is well characterized by a Gaussian function.

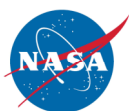
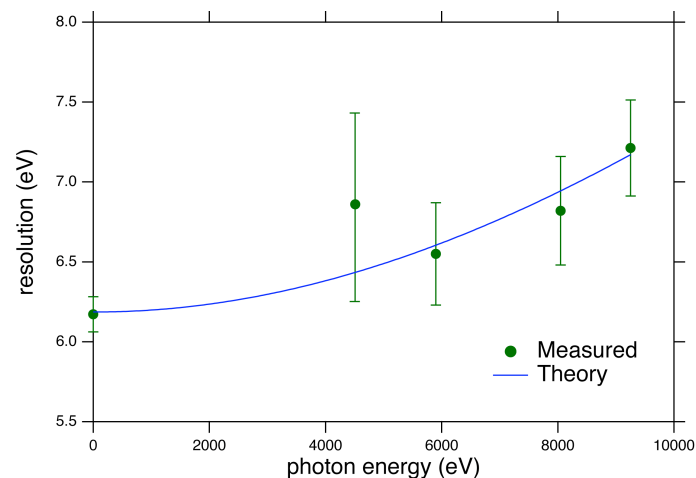
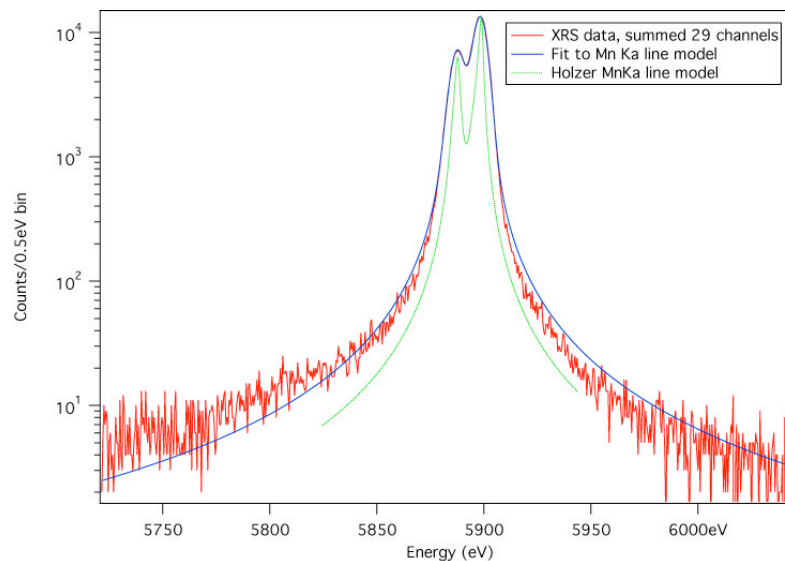
This resolution kernel is measured using a ^{55}Fe source. For the most flight-like conditions we find:

Composite: $\Delta E_{\text{FWHM}} \sim 5.6 \text{ eV}$

Pix mean: $\Delta E_{\text{FWHM}} \sim 5.3 \text{ eV}$

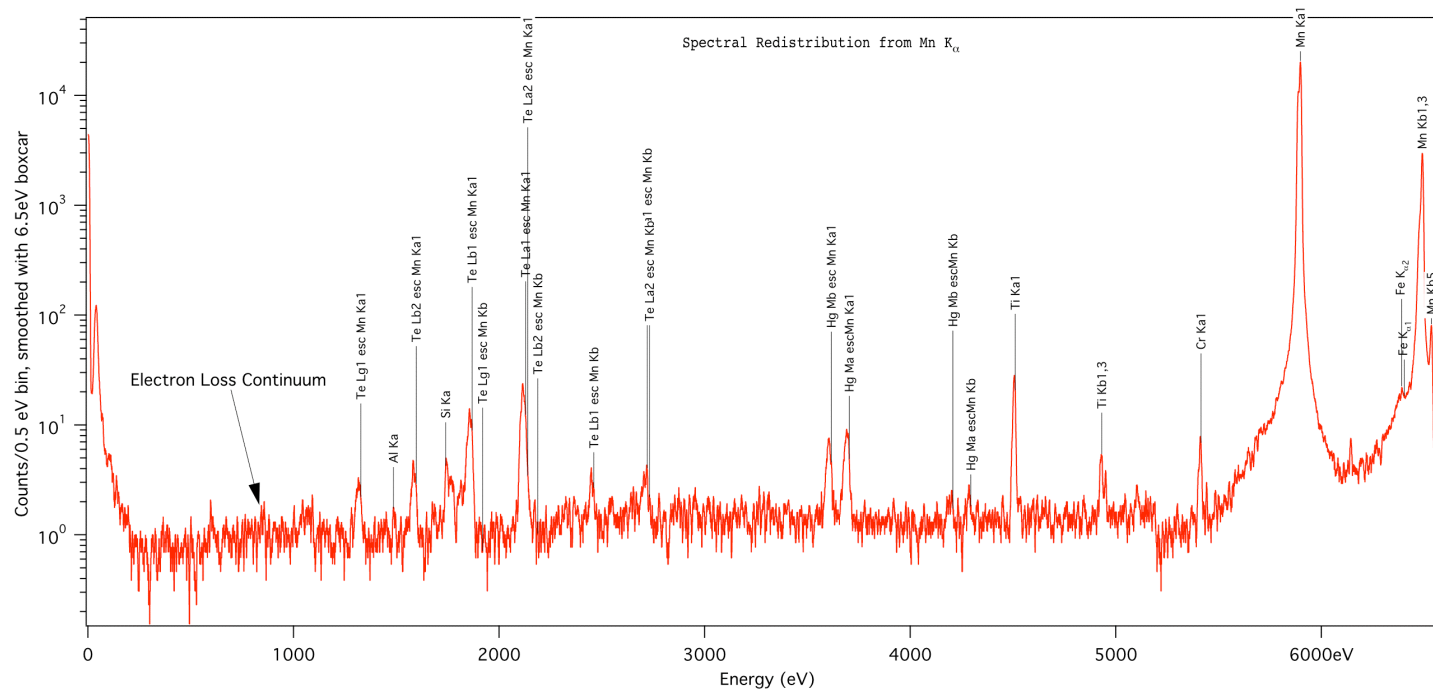
Std dev: $\sigma \sim 0.2 \text{ eV}$

The energy dependence appears to follow the predictions of the pulse model.



Line Spread Function: Low Energy Shoulder

There is a low energy shoulder due to photo- and electron-escape events. A monte-carlo is being developed. It depends on both the photoelectric absorption cross-sections and the electron interaction with the solid state HgTe absorber.



Effective Area

$$A_{\text{eff}} = A_{\text{tel}} * \eta_{\text{tel}} * \prod \eta_{\text{filters}} * \eta_{\text{intercept}} * \eta_{\text{QE}} * \eta_{\text{electronics}}$$

Telescope: Described by Kai-Wing Chan

Blocking Filters: Aluminum and oxides in the filters produce absorption structure at low energies. This is measured on the ground.

Pixel Intercept: This will depend on the boresight, the telescope PSF and the alignment of the pixels.

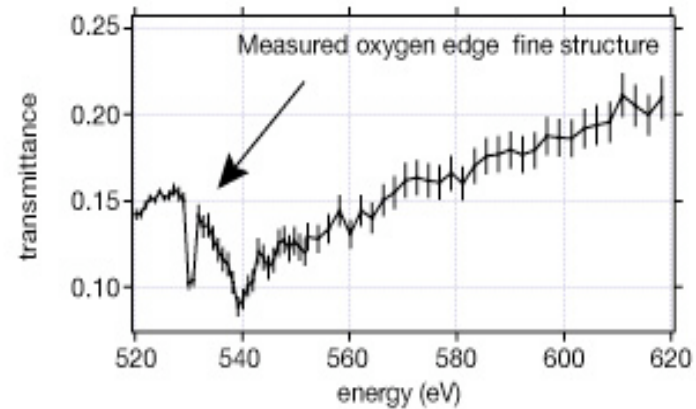
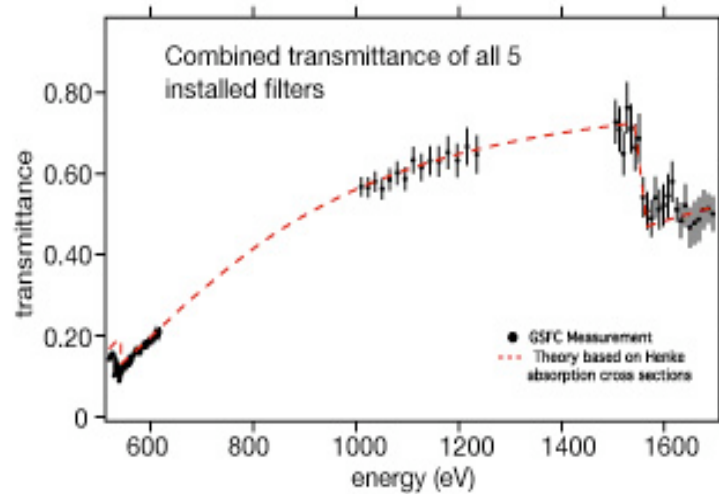
Absorber Quantum Efficiency: This depends on the column density of the HgTe absorbers. The absorbers have been measured and weighed, and the Hg L absorption edges have been measured.

Electronics: At high count rates some events will not be identified by the pulse detection algorithms. This 'pile up' will decrease the effective area by a few percent.

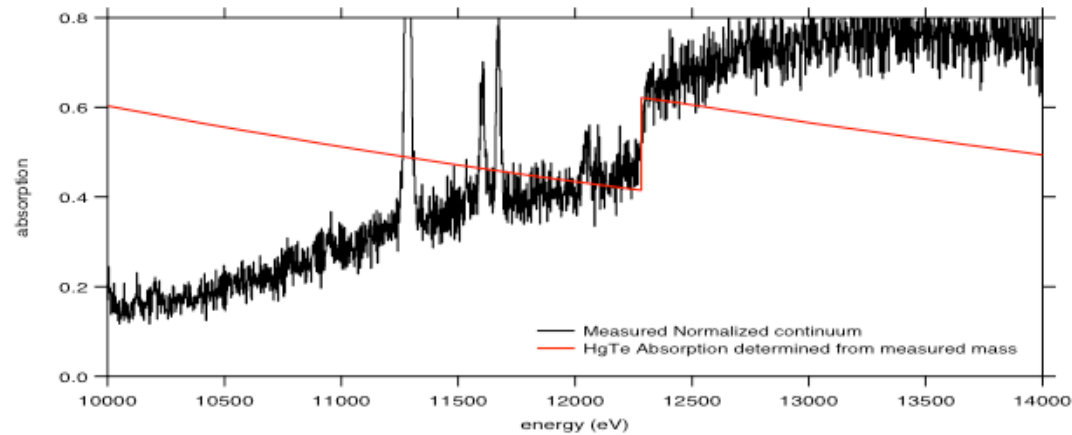


Effective Area: Components

Filter Transmission

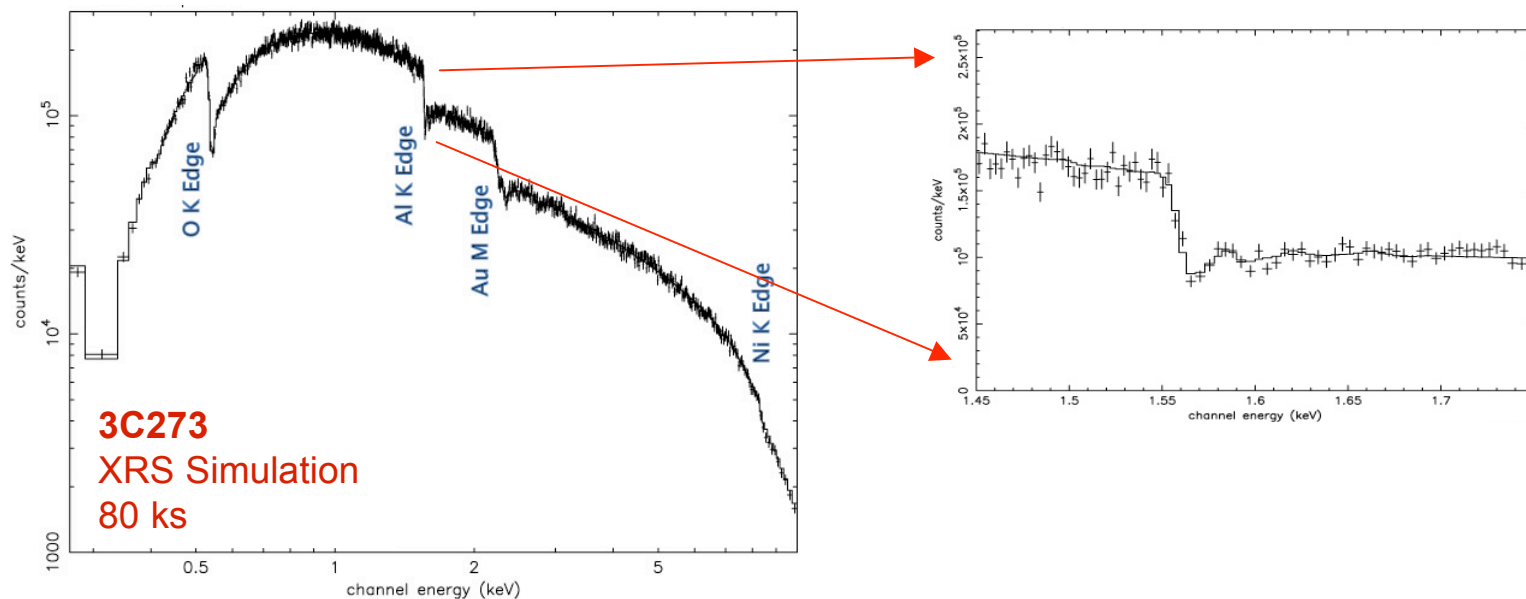


Quantum Efficiency

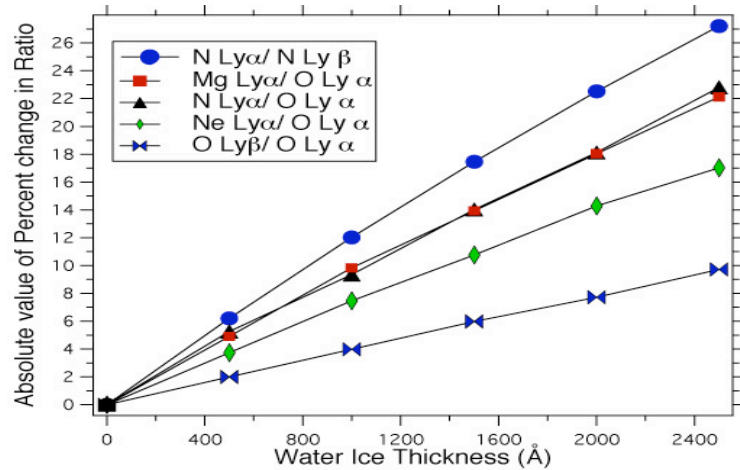


Effective Area: In-Flight

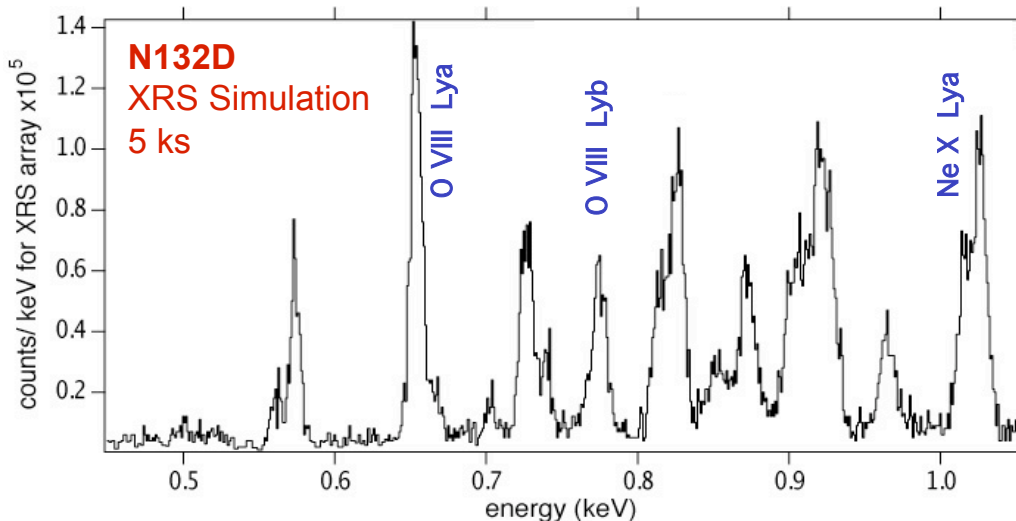
The goal of the in-flight calibration is to verify the discrete structure and characterize the global effective area. We will use the bright, featureless BL Lac **3C273** as a backlight. Simultaneous observations and cross-calibration with XMM-Newton/Chandra are required.



Effective Area: In-Flight



To monitor the presence of ice contamination on the blocking filters we will observe line-rich SNRs **N132D** and **1E0102-72** repeatedly during the early phases of the mission.



N132D		
Line	E (keV)	Cts
N VII Ly α	0.500	65
O VIII Ly α	0.654	1900
O VIII Ly β	0.775	850
Ne Ly α	1.022	2500
Mg Ly α	1.472	500

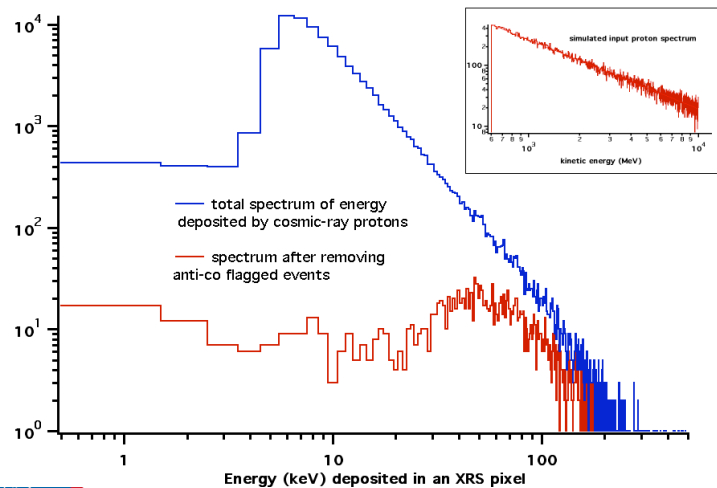


Background

Primary cosmic ray protons: The anticoincidence detector identifies all but ~0.1% of events due to primary protons. Protons that hit the frame cause simultaneous pulses on multiple pixels that can be rejected by the processing software.

Secondary electrons and photons: To estimate the unrejected background due to secondary events, we scale the ASCA rate $\rightarrow 7 \times 10^{-4}$ events/s.

Anti-Coincidence Detector Rejection



Simultaneous 'clustered' events

